

Pembrolizumab induces long term complete remission in patients with chemotherapy resistant gestational trophoblastic neoplasia despite classical HLA deficiency

Ehsan Ghorani MRCP^{1,2}, Baljeet Kaur FRCPath³, Rosemary A. Fisher PhD¹, Dee Short¹, Ulrika Joneborg PhD⁴, Joseph W. Carlson PhD⁵, Ayse Akarca BSc⁶, Teresa Marafioti PhD⁶, Sergio A. Quezada PhD², Naveed Sarwar PhD¹ and Michael J. Seckl PhD¹

1. Department of Medical Oncology, Charing Cross Gestational Trophoblastic Disease Centre, Charing Cross Hospital Campus of Imperial College London, UK.
2. Cancer Immunology Unit, University College London (UCL) Cancer Institute, London UK.
3. Department of Histopathology, Charing Cross Gestational Trophoblastic Disease Centre, Charing Cross Hospital Campus of Imperial College London, London, UK
4. Department of Women's and Children's Health, Karolinska Institutet, Karolinska University Hospital, Stockholm, Sweden.
5. Department of Oncology-Pathology, Karolinska Institutet, Karolinska University Hospital, Stockholm, Sweden.
6. Department of Cellular Pathology, UCL Hospital, London, UK

Correspondence Prof Michael Seckl, Department of Medical Oncology, Charing Cross Gestational Trophoblastic Disease Centre, Charing Cross Hospital Campus of Imperial College London, London W6 8RF, UK.

E-mail: m.seckl@imperial.ac.uk.

Telephone: +44 (0)20 3311 1421

Fax: +44 (0)20 8383 5577

Introduction

Gestational trophoblastic disease (GTD) is a spectrum of pregnancy related disorders ranging from pre-malignant hydatidiform mole through to malignant forms collectively referred to as gestational trophoblastic neoplasia (GTN). GTN includes the malignant invasive mole, choriocarcinoma and rare placental site trophoblastic and epithelioid trophoblastic tumours (PSTT/ETT).¹ Globally, approximately 18,000 women are diagnosed annually with GTN, most of whom are cured with chemotherapy guided by a sensitive disease response biomarker, human chorionic gonadotrophin (hCG). However, 0.5-5% of women die from multi-drug resistance, necessitating novel approaches. Risk factors for poor survival include drug refractory disease², liver and/or brain metastases^{3,4} and PSTT/ETT that develops four or more years after the antecedent pregnancy.⁵

Anti-cancer T-cell activity is regulated by multiple suppressive mechanisms, including tumour-expressed programmed death ligand 1 (PDL1) signalling to the T-cell inhibitory receptor PD1. Monoclonal antibodies to block this pathway, such as the anti-PD1 agent pembrolizumab, have shown impressive clinical activity in several cancer types.⁶

Placental expression of paternal antigens make this organ a target for maternal immune recognition during pregnancy and PDL1 expression maintains gestational tolerance. In pre-clinical models, loss of placental PDL1/PD1 signalling results in foetal rejection.⁷ PDL1 is strongly expressed by GTN⁸⁻¹⁰, suggesting its role in tumour immune-evasion. We therefore hypothesised that targeting PD-1 inhibitory signalling with pembrolizumab may be effective in drug resistant GTN. Here we report the outcomes of four patients treated across two European centres.

Cases

All patients had genetically verified gestational tumours (Table S1 and supplementary methods) with demographics summarised in Table S2. Patient 1 presented aged 39 with choriocarcinoma (Figure 1A) and multiple high risk factors including liver and brain metastases. At a second relapse three years later, she progressed through a fifth line of treatment including previous high dose chemotherapy (Figure 1B). Multiplex immunohistochemistry (IHC) on a chest wall biopsy revealed close to 100% tumour PDL1 expression, rich peritumoural and focal densities of tumour

infiltrating lymphocytes (TILs; Figure 1C and D) predominantly CD8⁺ cytotoxic T-cells, half of which were PD1⁺ (Figure 1H). Tumour cells were negative for the class I major histocompatibility complex (MHC-I) antigen HLA-A and MHC-II (Figure 1F-G) but positive for the immuno-inhibitory, non-classical MHC-I antigen HLA-G (Figure 1E). The serum hCG of 80 IU/L normalised to <5 IU/L after four cycles of pembrolizumab (3 mg/kg, every three weeks), that was discontinued after five further consolidation cycles. Residual liver lesions regressed on serial imaging and she remains in complete remission over 24 months later.

Patient 2 presented aged 44, 16 years after her last known pregnancy with uterine PSTT/ETT. Having failed multiple therapies over seven years (Figure S1A), tumour cells in the original hysterectomy sample and a lung metastasis biopsy were >90% PDL1 positive but TILs were absent (Figure S1B and C). Tumour cells were negative for HLA-A, pan-MHC-II and HLA-G (Figure S2D, E and data not shown). Reimaging after five cycles of pembrolizumab revealed disease progression in keeping with a rising serum hCG and she died four months later.

Patient 3 presented aged 47 with metastatic PSTT to the lung, liver and brain. Her brain metastases progressed during third line therapy (Figure S2A). Significant treatment related neuropathy precluded further chemotherapy. IHC on tissue fragments from a uterine biopsy revealed > 90% PDL1 staining and the presence of TILs. Tumour cells were negative for HLA-A and pan-MHC-II but positive for HLA-G. Upon commencing pembrolizumab, the serum hCG rose from 73 to 4476 IU/L before falling after four cycles. Re-imaging showed a partial response of the pulmonary metastases but multiple new brain lesions (Figure S2B and C). Her serum and cerebrospinal fluid hCG normalised after eight cycles. After five consolidation cycles, reimaging demonstrated residual uterine necrotic tissue only, confirmed pathologically. She remains in remission over 15 months following marker normalisation.

Patient 4 presented aged 37 with lung metastatic choriocarcinoma. She achieved remission after five lines of chemotherapy including high dose. IHC on a lung deposit revealed close to 100% tumour PDL1 expression with dense peri- and intratumoural foci of TILs, composed of approximately equal numbers of predominantly PD1 negative CD8⁺ and CD4⁺ helper T-cells with a high density of CD56⁺ natural killer (NK) cells. Tumour cells were HLA-A/MHC-II negative and HLA-G positive (Figure S1B-F and data not shown). On relapse five months later with lung and pelvic nodal disease, her hCG was 118 IU/L and pembrolizumab was commenced with marker normalisation after two cycles (Figure S3A). She received five consolidation courses and remains in remission over 5 months later.

Treatment was well tolerated in all cases with mild (grade 1-2) toxicities managed conservatively and details presented in Table S1.

Discussion

Patients with unresectable drug resistant GTN have a fatal outcome and anti-PD1 immunotherapy may be a life-saving treatment. The efficacy and favourable toxicity profile of pembrolizumab make its earlier use an attractive alternative to high dose chemotherapy. However, lasting fertility impairment due to persistent anti-trophoblast immunity is a concern that requires further study before offering therapy earlier in the treatment sequence.

As previously reported, we found GTN to strongly express PD-L1 that in this small sample was not a biomarker of response to immunotherapy. Features of the TIL landscape correlate with anti-PD1 response,¹¹ suggesting a causal link between TIL absence and outcome in the single non-responder.

Several cell types may mediate the effect of pembrolizumab on GTN rejection. Trophoblasts do not express the classical MHC-I molecules HLA-A/B, nor MHC-II, offering protection from T-cell mediated placental destruction.¹² We report that GTN is similarly negative for HLA-A and MHC-II. The strong presence of infiltrating T-cells in responders suggests pembrolizumab activation of HLA-C directed or indirect T-cell cytotoxicity. Effectors other than classically restricted T-cells may also be relevant. One candidate are NK cells that express PD-1, are cytotoxic towards classical MHC-I negative cells and are inhibited by HLA-G, that also acts to maintain gestational tolerance through mechanisms including T-cell suppression.¹³ Upregulated tumour expression of HLA-G by the responders suggests a role for this molecule in inhibiting infiltrating lymphocyte effectors. Beyond T-cell activation, the immune effects of pembrolizumab are not well understood but potentially of wider relevance, especially as HLA-G expression is a recognised mediator of tumour immune evasion.¹⁴

Complex restrictions precluded public funding of potentially life-saving off-label pembrolizumab for the UK treated patients 1-3. This report emphasizes the need to improve mechanisms for funding rare disease treatments, for which randomised trials and established licencing pathways are not feasible. Based on the evidence presented here, UK public funding of pembrolizumab for drug resistant GTN is now under review.

In summary, we provide evidence in favour of pembrolizumab as an important advance in the management of drug resistant GTN that should strongly be considered in this setting. Tumour infiltrating lymphocytes and HLA-G expression may identify responders and our analysis of

MHC expression suggests potential effects of pembrolizumab on cell types other than classically restricted T-cells.

Acknowledgements: Professor Seckl would like to thank the continued support of the UK Dept of Health for the funding of the Gestational Trophoblastic Disease Service.

Funding: EG is funded by a Wellcome Trust Research Training Fellowship and an NIHR Fellowship. MJS and RAF acknowledge support from CRUK, Department of Health, Imperial College Experimental Cancer Medicine Centre and NIHR Biomedical Research Centre. The Harris and Trotter Clients Charitable Trust funded therapy for two patients.

Author contributions: EG, BK, TM, SAQ and MJS designed the study. EG, UJ, NS and MJS enrolled patients and participated in clinical data collection. BK, JWC, TM and AA carried out immuno-stains and pathological review. EG, BK, JWC, TM, RF, UJ, SAQ, NS and MJS contributed to data analysis and interpretation. RF and JWC carried out genetic analyses. DS provided administrative support. EG, AA, RF, UJ and MJS wrote the report. All authors have seen and approved the final version.

References

- 1 Seckl MJ, Sebire NJ, Berkowitz RS. Gestational trophoblastic disease. *Lancet (London, England)* 2010; **376**: 717–29.
- 2 Powles T, Savage PM, Stebbing J, *et al.* A comparison of patients with relapsed and chemo-refractory gestational trophoblastic neoplasia. *Br J Cancer* 2007; **96**: 732–7.
- 3 Ahamed E, Short D, North B, Savage PM, Seckl MJ. Survival of women with gestational trophoblastic neoplasia and liver metastases: is it improving? *J Reprod Med*; **57**: 262–9.
- 4 Savage P, Kelpanides I, Tuthill M, Short D, Seckl MJ. Brain metastases in gestational trophoblast neoplasia: an update on incidence, management and outcome. *Gynecol Oncol* 2015; **137**: 73–6.
- 5 Schmid P, Nagai Y, Agarwal R, *et al.* Prognostic markers and long-term outcome of placental-site trophoblastic tumours: a retrospective observational study. *Lancet (London, England)* 2009; **374**: 48–55.
- 6 Herbst RS, Baas P, Kim D-W, *et al.* Pembrolizumab versus docetaxel for previously treated, PD-L1-positive, advanced non-small-cell lung cancer (KEYNOTE-010): a

- randomised controlled trial. *Lancet (London, England)* 2016; **387**: 1540–50.
- 7 Guleria I, Khosroshahi A, Ansari MJ, *et al.* A critical role for the programmed death ligand 1 in fetomaternal tolerance. *J Exp Med* 2005; **202**: 231–7.
 - 8 Veras E, Kurman RJ, Wang T-L, Shih I-M. PD-L1 Expression in Human Placentas and Gestational Trophoblastic Diseases. *Int J Gynecol Pathol* 2016; published online June 29. DOI:10.1097/PGP.0000000000000305.
 - 9 Bolze P-A, Patrier S, Massardier J, *et al.* PD-L1 Expression in Premalignant and Malignant Trophoblasts From Gestational Trophoblastic Diseases Is Ubiquitous and Independent of Clinical Outcomes. *Int J Gynecol Cancer* 2017; **27**: 554–61.
 - 10 Inaguma S, Wang Z, Lasota J, *et al.* Comprehensive Immunohistochemical Study of Programmed Cell Death Ligand 1 (PD-L1). *Am J Surg Pathol* 2016; **40**: 1133–42.
 - 11 Tumeh PC, Harview CL, Yearley JH, *et al.* PD-1 blockade induces responses by inhibiting adaptive immune resistance. *Nature* 2014; **515**: 568–71.
 - 12 Moffett A, Chazara O, Colucci F. Maternal allo-recognition of the fetus. *Fertil Steril* 2017; **107**: 1269–72.
 - 13 Waldhauer I, Steinle A. NK cells and cancer immunosurveillance. *Oncogene* 2008; **27**: 5932–43.
 - 14 Urosevic M, Dummer R. Human Leukocyte Antigen-G and Cancer Immunoediting. *Cancer Res* 2008; **68**: 627–30.

Figure 1. Genetics, treatments, response and immune phenotyping for Patient 1

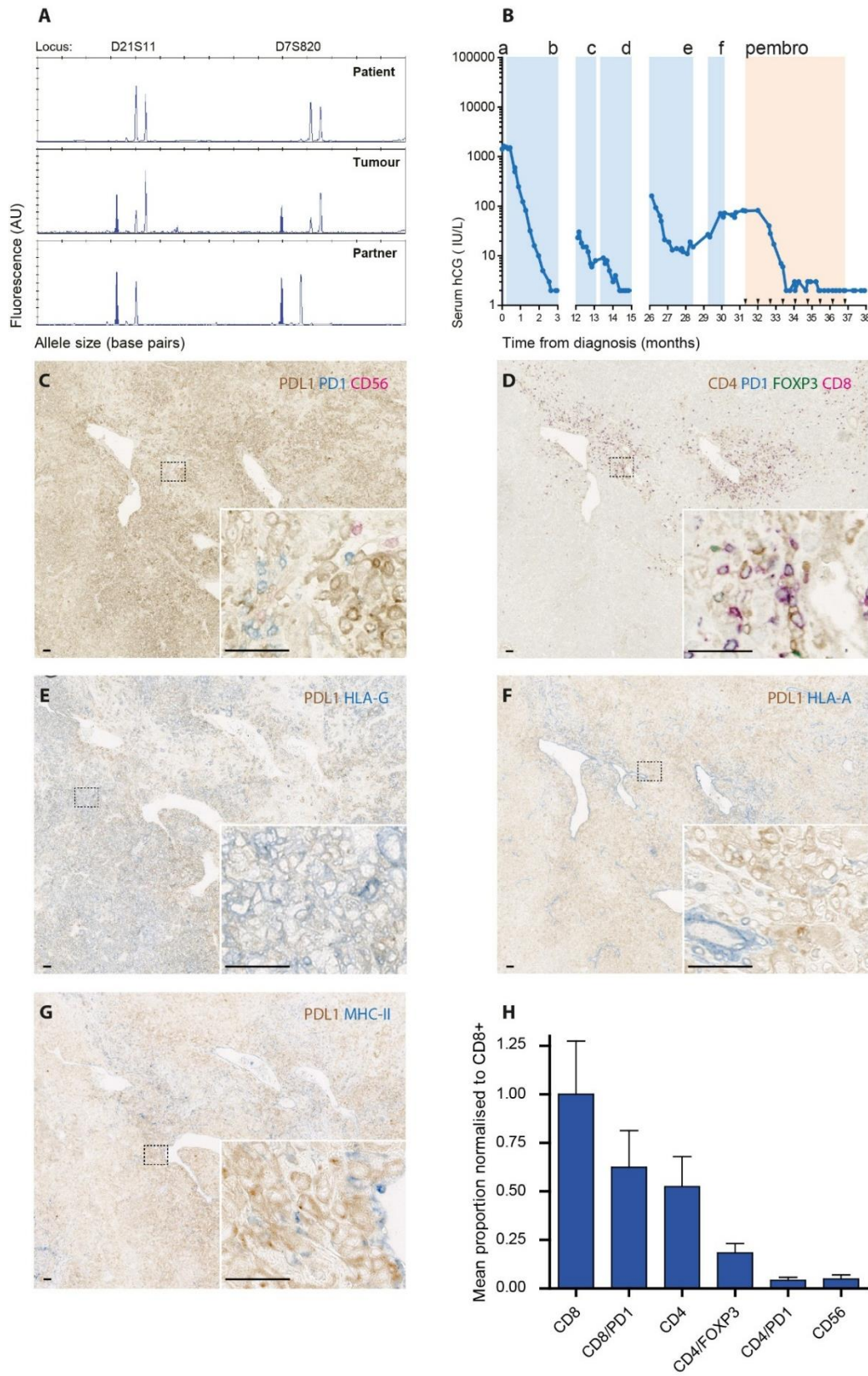


Figure 1. (A) Partial electropherograms of DNA from patient 1, her partner and tumour tissue. Genotyping of the tumour for short tandem repeat loci D21S11, D7S820 (shown) demonstrates a single non-maternal allele (solid peak) representing a contribution to the tumour genome from the partner. Both maternal alleles (open peaks) are present in the tumour DNA, the lower open peak (left) representing contamination from maternal cells in the tumour sections, while the higher open peak (right) represents a maternal contribution to the tumour genome plus a small proportion of contamination from maternal cells in the tumour sections. (B) Serum hCG is plotted against time from treatment initiation. Shaded bands represent duration of chemo- and immunotherapy with; a. Low dose EP; b. EP/EMA with IT MTX; c. TE/TP; d. HDCT; e. EP; f. Gem-TIP; Pembro, pembrolizumab (arrowheads show treatment dates). See Table S2 for a summary of therapeutic regimens. (C-F) Multiplex immunohistochemistry of the tumour immune landscape. (C) Expression of PDL1 and tumour infiltrating lymphocyte (TIL) expression of the activation/exhaustion marker PD1 and CD56 expressing natural killer cells; (D) TIL expression of CD4, PD1, FOXP3 (regulatory T-cells that co-express CD4) and CD8; (E-G) tumour expression of HLA-G, HLA-A and MHC-II. The latter three markers were counterstained for PDL1 expression to identify tumour cells. Normal HLA-A/MHC-II expression is seen on non-cancer cells including endothelial cells and lymphocytes, bars represent 50 μ m. (H) TILs in three areas comprising one third of the tumour were digitally and manually counted and the mean proportions normalised to CD8 T-cells. Error bars represent one standard deviation from the mean.

Supplementary data

Materials and methods

Multiplex immunohistochemistry

Tumour samples and reactive human tonsil tissue were fixed in 10% buffered formalin and embedded in paraffin according to standard protocols. 2-5µm tissue sections were cut and transferred onto poly-l-lysine-coated slides, dewaxed in two changes of xylene and rehydrated in a series of graded alcohols. Single immunohistochemistry was carried out using the automated platforms BenchMark Ultra (Ventana/Roche) and the Bond-III Autostainer (Leica Microsystems) according to a protocol described elsewhere.^{1,2} To establish optimal staining conditions each antibody was tested and optimized on sections of human reactive tonsil, used as positive control. Monoclonal antibodies used were as follows; anti-CD4 (Spring Biosciences, clone SP35), anti-CD8 (Spring Biosciences, clone SP239), anti-PD1 clone NAT 105/E3 and anti-FOXP3 clone 236/E7 (kindly gifted by Dr. G. Roncador), anti-CD56 clone CD564 (Leica Microsystems), anti-HLA-A clone EP1395Y, anti-HLA-G clone 4H84 and anti-pan-MHC-II clone CR3/43 (Abcam). Anti-PDL1 clone SP263 (Ventana) was used to score tumour PDL1 status, whereas anti-PDL1 clone QR1 (Quarttet) was used to identify tumour cells in dual staining with anti-MHC antibodies.

Multiplex immunohistochemistry was carried out using a protocol described previously.³ Specificity of the staining was assessed by a haematopathologist (TM) with expertise in multiplex-immunostaining. Slides were scanned using the Hamamatsu Nanozoomer Digital scanner. Staining was independently reviewed by a second pathologist with expertise in GTD (BK). Cell counts for Patient 1 were determined in ImageJ using automatic and manual methods.

Fluorescent microsatellite genotyping of tumour tissue.

In each case tumour and surrounding host tissue were independently microdissected from formalin-fixed, paraffin-embedded (FFPE) pathological sections of tumour tissue, with reference to a haematoxylin and eosin stained section. DNA was prepared from tumour and host tissue in all cases using a QIAmp DNA FFPE Tissue Kit (Qiagen; cases 1-3) or a PicoPure DNA extraction kit (Arcturus; case 4) and from blood samples from the patient and her partner in case 1 and 3. DNA was amplified with primers for 15 short tandem repeat (STR) loci on 13

chromosomes, together with the amelogenin locus, using an AmpFISTR Identifiler Plus kit (Applied Biosystems; cases 1-3) or 9 STR using an AmpFISTR Profiler Plus. Kit (Applied Biosystems; case 4). PCR products were resolved by capillary electrophoresis using an ABI 3100 or 3500 Genetic Analyser and genotypes determined using GeneMapper version 5.0 (Applied Biosystems) or GeneMarker version 2.4 software (SoftGenetics LLC). Demonstration of the presence of paternal alleles, or non-maternal alleles in cases 2 and 4 in DNA from the tumour confirmed a diagnosis of gestational trophoblastic neoplasia.

References

- 1 Marafioti T, Paterson JC, Ballabio E, *et al.* Novel markers of normal and neoplastic human plasmacytoid dendritic cells. *Blood* 2008; **111**: 3778–92.
- 2 Akarca AU, Shende VH, Ramsay AD, *et al.* BRAF V600E mutation-specific antibody, a sensitive diagnostic marker revealing minimal residual disease in hairy cell leukaemia. *Br J Haematol* 2013; **162**: 848–51.
- 3 Marafioti T, Jones M, Facchetti F, *et al.* Phenotype and genotype of interfollicular large B cells, a subpopulation of lymphocytes often with dendritic morphology. *Blood* 2003; **102**: 2868–76.

Table S1. Genotyping of patient, tumour and partner tissue confirms gestational origin of the tumour

Locus:	D8S1179	D21S11	D7S820	CSF1PO	D3S1358	THO1	D13S317	D16S539	D2S1338	D19S433	vWA	D18S51	D5S818	FGA
Patient 1														
Patient	11	29 - 30	11 - 12	9 - 14	14 - 18	8 - 9	9 - 11	9 - 11	18 - 20	14.2 - 16	17 - 18	15 - 17	10 - 11	19 - 22
Tumour	11	27 - 30	8 - 12	9 - 10	18	6*	9 - 13	10 - 11	20	14.2-15.2	17 - 18	15 - 18	10 - 13	26*
Partner	10 - 11	27 - 29	8 - 10	10	14 - 18	6 - 8	13	8 - 10	19 - 20	14.2-15.2	17 - 18	18	11 - 13	20 - 26
Patient 2														
Patient	10 - 13	30 - 31	9 - 11	12	15 - 18	6 - 7	11 - 16	9 - 10	17 - 20	14	14 - 17	12 - 17	11 - 12	18 - 22
Tumour	10 - 15	31 - 31.2	9 - 10	12	15 - 17	6 - 9	10 - 16	9 - 11	17	14 - 16.2	17	16 - 17	11	18 - 20
Patient 3														
Patient	12	31 - 32.2	11	10 - 11	15	9	11 - 16	9	20 - 21	13 - 15	14	14 - 15	11	23 - 24
Tumour	12*	30 - 31	8 - 11	N/S	15 - 17	9	11 - 16	9 - 12	21 - 25	N/S	14 - 16	14 - 15	11	19 - 24
Partner	10 - 15	30	8 - 10	11 - 12	17	9 - 9.3	11 - 16	11 - 12	22 - 25	13	16 - 17	15 - 20	10 - 11	19
Patient 4														
Patient	12	N/S	8 - 9	N/D	16 - 18	N/D	9 - 11	N/D	N/D	N/D	17 - 20	18 - 18.2	10 - 11	22 - 25
Tumour	11 - 12	N/S	8 - 11	N/D	16 - 19	N/D	9 - 12	N/D	N/D	N/D	16 - 17	18	11 - 12	21 - 25

Numbers represent alleles identified for informative tandem repeat loci and the amelogenin locus. Genotypes at the TPOX locus were uninformative in all cases. All tumours had a single sex chromosome specific peak representing DNA from the X chromosome. * Loci for which loss of heterozygosity was observed in cases 1 and 3; N/S, not scored. N/D, not done. DNA was not available for the partner of Patients 2 and 4.

Table S2. Summary of patient baseline characteristics and prior therapies.

	Patient 1	Patient 2	Patient 3	Patient 4
Age ¹	42	52	48	37
Performance status ¹	0	2	1	0
Obstetric status	G2P2	G3P3	G3P2	G2P2
GTN subtype	CC	ETT (predominant)/PSTT	PSTT	CC
Antecedent pregnancy (years)	3	16	11	0.75
Sites of disease	Nodal, hepatic	Nodal, hepatic, pulmonary, pleural	Pelvic, hepatic, pulmonary, brain	Nodal, hepatic
Disease duration (years)	2.6	7.8	0.6	1.25
FIGO score at diagnosis	17	8	20	6
Prior chemotherapy (cycles)				
1	Induction EP (1)	EP/EMA (8)	Induction EP (3)	IM MTX (2)
2	EP/EMA CNS (8), IT MTX (2)	TE/TP (4)	EP/EMA CNS (5), IT MTX (3)	EMA/CO (8) IT MTX (3)
3	TE/TP (4)	-	TE/TP (4) IT MTX (3)	TE/TP (2) EP/EMA (1)
4	HDCT (2)	-	Escalated EP (5), IT MTX (8)	HDCT (2)
5	Escalated EP (6)	-	-	-
6	Gem-TIP (2)	-	-	-
Prior surgery	TM	HBSO, TM	-	TM
Serum hCG	80	2468	73	118
Biochemical response and duration (months)	CR (24)	PD	CR (15)	CR (5)
Radiological response	Ongoing PR	PD	Ongoing PR	Ongoing PR
Pembrolizumab				
Cycles to hCG normalisation	4	-	8	2
Consolidation cycles	5	-	5	5
Adverse events (grade)	Arthralgia (1)	Pruritis (1)	Synovitis (2), rash (1)	Neutropaenia (2), synovitis (1)

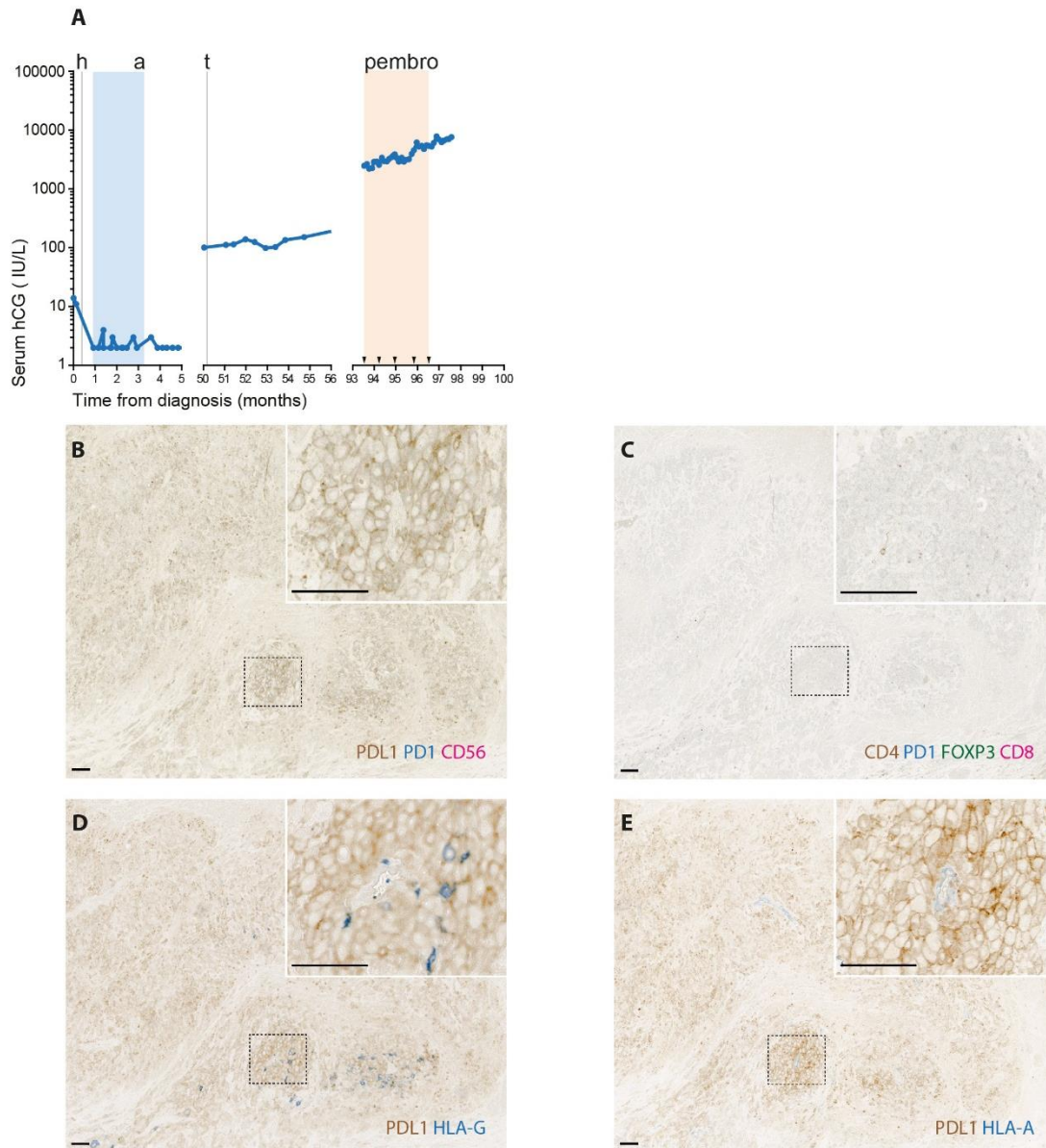
¹Age or performance status at commencement of pembrolizumab. TM, thoracic metastasectomy; HBSO, hysterectomy and bilateral salpingo-oophorectomy; G (gravida); P (para). CR, complete response; PD, progressive disease; PR, partial response. Adverse events were graded according to the Common Terminology Criteria for Adverse Events (CTCAE) v4.03. Radiological responses were evaluated according to Response Evaluation Criteria In Solid Tumors (RECIST) v1.1. Details of chemotherapeutic regimens are given in Table S3.

Table S3. Treatment regimens

Regimen and cycle length (weeks)	Agent and dose
Pembrolizumab ^a (3)	3 mg/kg pembrolizumab D1
IM MTX (2)	50 mg methotrexate D1, 3, 5, 7
EMA/CO (2)	
EMA	0.5 mg actinomycin D1, 2
	100 mg/m ² etoposide D1, 2
	300 mg/m ² methotrexate D1
CO	1 g/m ² vincristine D8
	600 mg/m ² cyclophosphamide D8
Induction EP (1)	100 mg/m ² etoposide D1, 2
	20 mg/m ² cisplatin D1, 2
EP/EMA CNS ^b (2)	
EMA	0.5 mg actinomycin D1, 2
	100 mg/m ² etoposide D1, 2
	1000 mg/m ² methotrexate D1
EP	150 mg/m ² etoposide D8
	75 mg/m ² cisplatin D8
IT MTX (2)	12.5 mg methotrexate D1
TE/TP ^c (4)	
TE	150 mg/m ² etoposide D1
	135 mg/m ² paclitaxel D1
TP	60 mg/m ² cisplatin D14
	135 mg/m ² paclitaxel D14
Escalated EP (2)	500mg/m ² etoposide D1
	60mg/m ² cisplatin D1
Gem-TIP (3)	1200 mg/m ² gemcitabine D1
	175 mg/m ² paclitaxel D1
	1000 mg/m ² ifosfamide D2-6
	20 mg/m ² cisplatin D2-6
HDCT	75 mg/m ² paclitaxel D-7, -5, -3
	450 mg/m ² etoposide D-7, -5, -3
	AUC 10 carboplatin D-7, -5, -3
	60 mg/kg cyclophosphamide D-5, -3
	Autologous haematopoietic stem cells D0

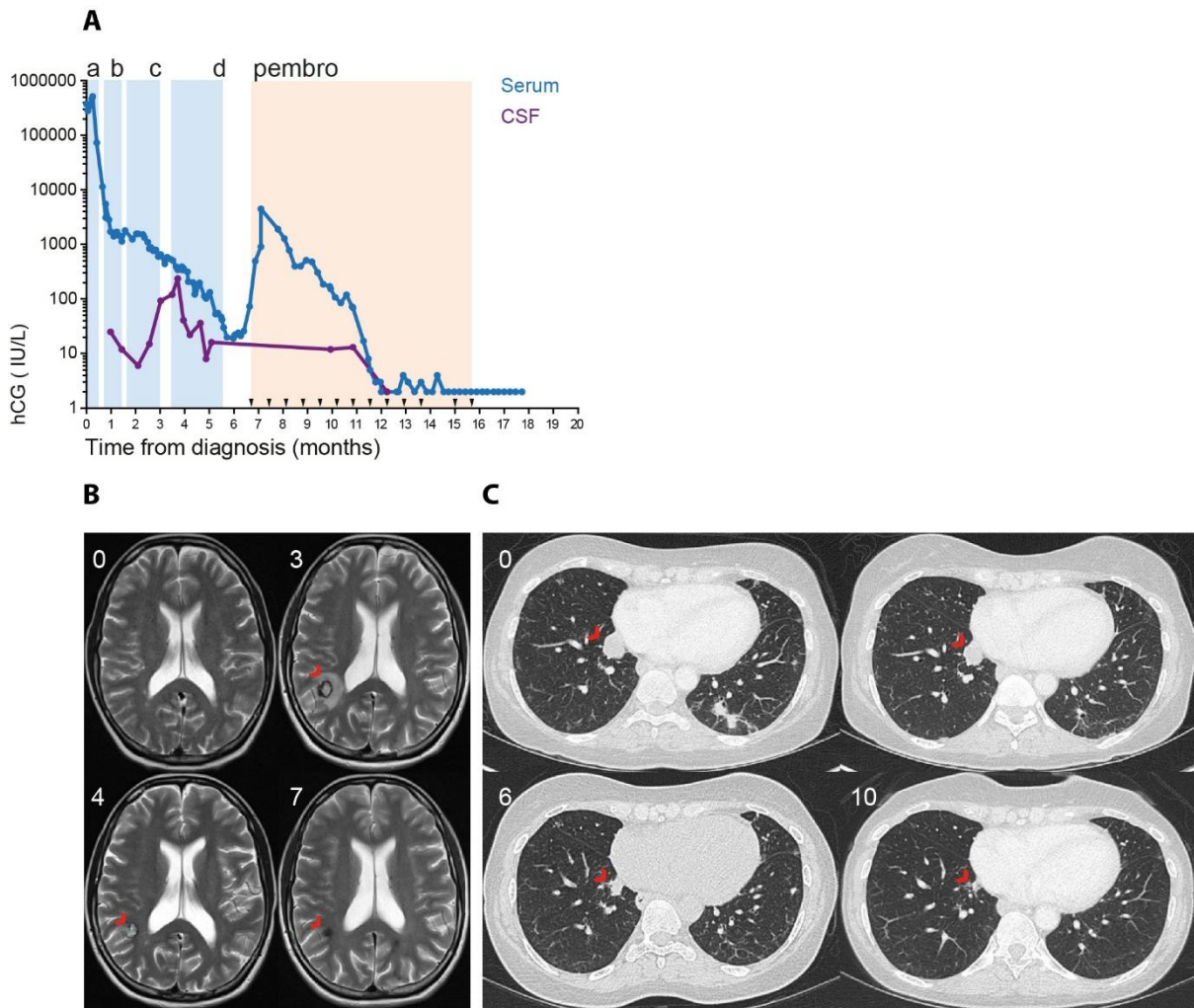
IM, intramuscular; IT, intrathecal; D, day; AUC, area under the concentration-time curve. a. Patient 4 received pembrolizumab 200 mg every 2 weeks. b. For Patient 1, carboplatin AUC 4 was substituted for cisplatin. Patient 2 received 300 mg/m² methotrexate. c. For Patient 1, carboplatin AUC 4 was substituted for cisplatin.

Figure S1. Treatments, response and immune phenotyping for Patient 2



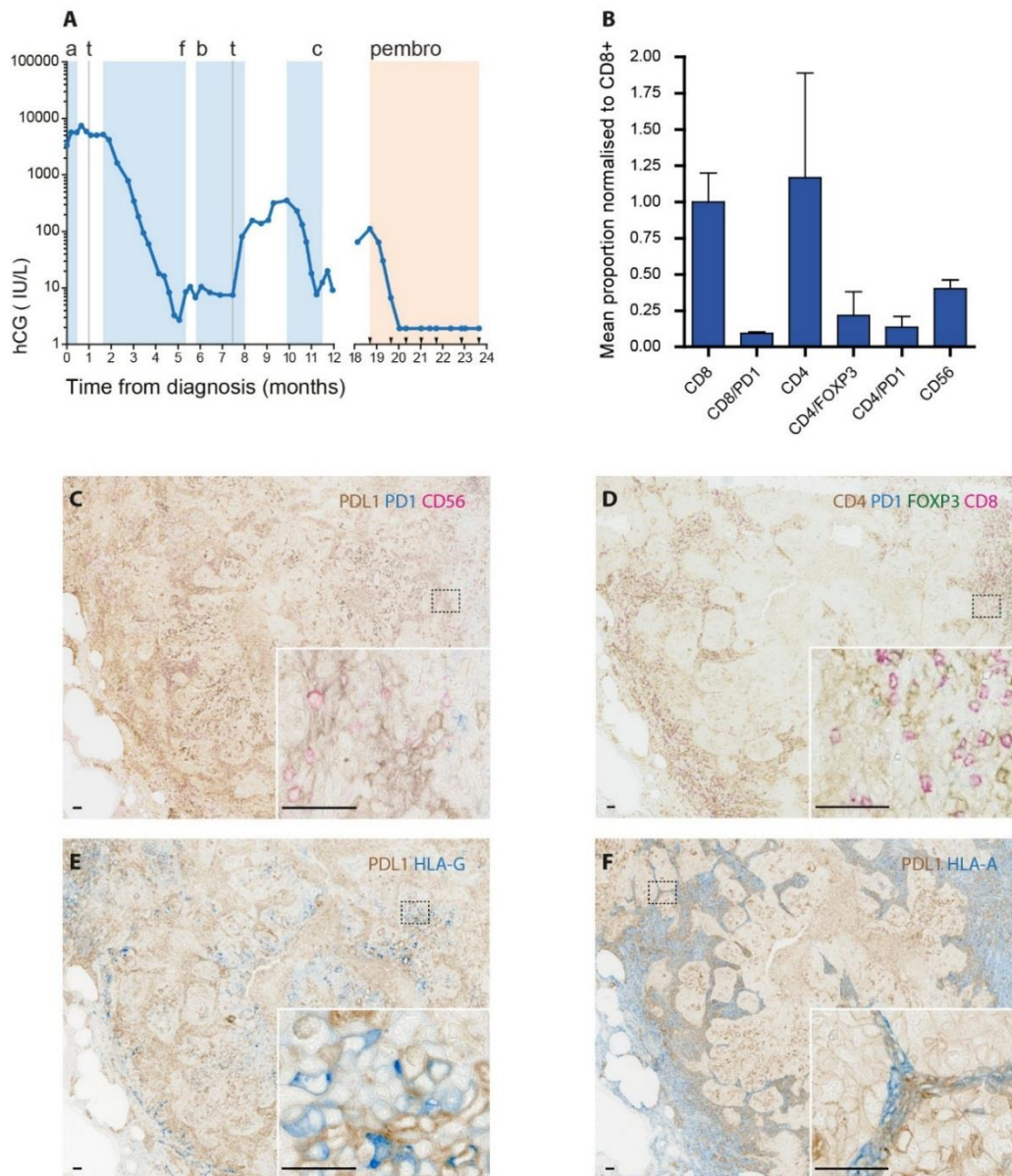
(A) Serum hCG is plotted against time from treatment initiation. Shaded bands represent duration of chemo- and immunotherapy with; a. EP/EMA; Pembro, pembrolizumab (arrowheads show treatment dates). H, hysterectomy; t, thoracic metastasectomy. TE/TP was additionally given prior to pembrolizumab at another institution (data not shown), see Table S2 for a summary of therapeutic regimens. (B-E) Multiplex immunohistochemistry on the uterine primary showing staining for PDL1, PD1 and CD56 (B); CD4, PD1, FOXP3 and CD8 (C); HLA-G (D) and HLA-A (E). The latter two were counterstained for PDL1 expression to identify tumour cells. Normal HLA-A expression is seen on non-cancer cells including endothelial cells and lymphocytes, and HLA-G expression is seen on non-tumour infiltrating cells. Bars represent 100 μ m.

Figure S2. Treatments, response and imaging for Patient 3



(A) Serum hCG is plotted against time from treatment initiation. Shaded bands represent duration of chemo- and immunotherapy with; a. Induction EP; b. EP/EMA CNS; c. TE/TP; d. Escalated EP; Pembro, pembrolizumab (arrowheads show treatment dates). For treatments b-d, IT MTX was given concurrently. See Table S2 for a summary of therapeutic regimens. Serum (blue) and cerebrospinal fluid (CSF; purple) hCG response is shown. (B-C) Radiological response to pembrolizumab. (B) Serial contrast enhanced MRI head scans show flare and resolution of a brain metastasis. (C) Serial CT chest imaging shows resolution of a lung metastasis. Numbers represent months following initiation of pembrolizumab therapy (t=0 represents baseline imaging).

Figure S3. Treatments, response and immunophenotyping for Patient 4



(A) Serum hCG is plotted against time from treatment initiation. Shaded bands represent duration of chemo- and immunotherapy with; a. IM MTX; b. EMA/CO and IT MTX; c. TE/TP (and a single cycle of EP/EMA); d. HDCT; Pembro, pembrolizumab (arrowheads show treatment dates). t, thoracic metastasectomy. See Table S2 for a summary of therapeutic regimens. (B) Tumour infiltrating lymphocytes (TILs) in three areas comprising one third of the tumour were manually counted and the mean proportions normalised to CD8 T-cells. Error bars represent standard deviation. (C-F) Multiplex immunohistochemistry showing expression of PDL1, the activation/exhaustion marker PD1 and CD56 expressing natural killer cells (C); phenotype of TILs stained for CD4, PD1, FOXP3 (regulatory T-cells that co-express CD4) and CD8 (D); tumour HLA-G (E) and HLA-A (F). The latter two were counterstained for PDL1 expression to identify tumour cells. Normal HLA-A expression is seen on non-cancer cells predominantly representing stromal and inflammatory cells, bars represent 50 μ m.